The structural phase transition, degree of polymerization and dynamics characteristics of liquid magnesium silicate. A molecular dynamics simulation

ABSTRACT

In this paper, we report on the structural phase transitions, degree of polymerization, and dynamics characteristics in liquid magnesium silicate (Mg_2SiO_4) under pressure of molecular dynamics (MD) simulation. The results indicate that the structure of Mg_2SiO_4 liquid includes MgO_y (y = 3, 4,…8) basic units distributed in the Si-O structure network that powerfully depend on pressure. In the range 28-32 GPa, the Si-O structure network causes structural transformation from SiO_4 to SiO_6 via SiO_5 units. Mg-O and Si-O subnets tend to form clusters with structural heterogeneity. The degree of polymerization is considered via characteristics of OT_2 (T is Si or Mg), triclusters, tetraclusters bonds, and the cluster of MgO_y-MgO_y, SiO_x-SiO_x and MgO_y-SiO_x links. We find that the degree of polymerisation significantly increases under compression. The dynamic in Mg_2SiO_4 liquid has been investigated through the self-diffusion, low and fast atoms. Besides, we also focus on finding evidence about the fast diffusion of Mg atoms in a low-pressure range.

KEYWORDS: Mg_2SiO_4 liquid, structural phase transition, dynamics characteristics, dynamics heterogeneity, polymerization.

I. INTRODUCTION

Olivine and its polymorphs of dominantly magnesium silicate (Mg_2SiO_4) composition make up approximately 60% of the Earth's upper mantle and transition zone. Therefore, Mg_2SiO_4 liquid plays a disproportionately large role in our understanding of terrestrial chemical and thermal evolution. That is key to predicting properties at conditions previously unexplored, and also offers deep insight into the physics of the liquid state. To accurately describe these processes, knowledge of the changes in liquid physical properties with pressure and temperature is needed. In addition, Mg_2SiO_4 can be used as a glidant, anti-caking agent, a carrier for fragrances and flavors in the pharmaceutical industry and in food products [1,2]. Besides, Mg_2SiO_4 is used as a filler for many silicone and rubber products [3,4]. Mg_2SiO_4 liquid has attracted the attention of researchers over the past few decades. This material is refractory and is difficult to measure its structures and structure-dependent properties. That has led to extrapolations of properties from supercooled liquids to high temperatures or extrapolation from other compositions to Mg_2SiO_4. The structure of Mg_2SiO_4 glasses has been determined using combined neutron and high-energy diffraction and shows changes in the short-range order as a function of composition. These changes include a jump in Mg–O coordination number at the limit to the formation of the silicate network in forsterite composition glass. These results imply a similar change in the structure of the liquid. Mg_2SiO_4 liquid is interpreted as forming a relatively 'fragile' network of SiO_4 tetrahedra and

dominated by MgO_n (n = 4, 5, 6) polyhedra and highly mobile oxygen ions. The SiO_4 tetrahedral unit consists of one central Si atom and four surrounding oxygen atoms. They are linked together through the common oxygen atom (bridged oxygen-BO). In addition, this material contains non-bridged oxygen atoms. In ref. [5-11] have shown that the bond distance of Mg-O to be 1.83 - 2.0 Å, Si-O to be 1.60 - 1.64 Å, the Si–O and Mg-O coordination numbers are 4.1 – 6.0 and 5.0 – 7.7, respectively. Changes in physical properties must be caused by structural changes in the melt that are difficult to monitor experimentally. For a quantitative analysis using nuclear magnetic resonance for ^{27}Al, ^{29}Si or ^{17}O [12-14] samples must be synthesized at high pressure and temperature, and the quenched glass can then be analyzed at room pressure. Alternatively, the structural properties of Mg_2SiO_4 were studied by X-ray diffraction and neutron scattering and reveal structural correlations between different components. Such studies on Mg_2SiO_4 [12] reveal that glass/melt connectivity result from Mg–O polyhedra. SiO_4 units, that typically serve as network formers, show almost no connectivity, with Si_2O_7 dimers (Q1 species) coexisting with isolated SiO_4 units (Q0 species). In analogy to the crystalline phases, connectivity in the melt and coordination of Si can be expected to increase with pressure, but quantitative experiments to this extent have not been performed to date. In light of these difficulties numerous molecular dynamics simulations on structure and physical properties of silicate melts have been. The results showed that while Si stays overwhelmingly in tetrahedral coordination, the coordination of Mg increases significantly under compression, from an average 5-fold coordination at room pressure to 7-fold coordination at 24GPa. Medium range order in Mg_2SiO_4 changes considerably with pressure. Diffusivity of the atomic species in Mg_2SiO_4 decreases uniformly with pressure and viscosity a rapid increase with pressure. Ionic or atomic diffusion controls the kinetics of many physical and chemical processes in Earth's mantle, such as, chemical heterogeneities and electrical conductivity. Thus, understanding and quantifying these processes in Earth requires knowledge of diffusion coefficients for mantle minerals over the range of pressure–temperature conditions encompassed by Earth's mantle. Dobson et al. [15] reported that oxygen self-diffusion is two orders of magnitude faster than Si self diffusion in $MgO\text{-}SiO_2$ perovskite at 25 GPa and temperature ranging from 1673 to 2073 K. Baohua Zhang et al investigated the dependences of temperature and pressure on the self-diffusion coefficients of Mg_2SiO_4. The pressure dependence of viscosity with an exponential function, increasing with pressure [16]. Experimental estimates on melt viscosity for depolymerized melts, where for both diopside [17] and peridotite [18] viscosity initially increase with pressure, then decrease. In [18] the initial increase was attributed to a redistribution of inter tetrahedral angle, while the subsequent decrease was interpreted as an increase in coordination of network-forming cations. However, authors do not find any indication of sudden changes in coordination [7], but a continuous change, as many other computational studies [6,19-21] although to a smaller extent. As in the case for solid Mg_2SiO_4, the network modifying ion (Mg) diffuses much faster than the network forming cation (Si): $D_{Mg} \gg D_O \gg D_{Si}$. The diffusion coefficients decrease with pressure [7].

II. COMPUTATIONAL PROCEDURE

MD simulation were performed on Mg_2SiO_4 models containing 4998 atoms (714 Si, 2856 O, and 1428 Mg atoms). The Oganov pairwise potentials and periodic boundary conditions were used to build the models. Oganov potentials have been effectively employed to

simulate the structure and dynamics of magnesium silicate systems (both in glass and melt states) were applied to construct Mg_2SiO_4 models at 3500 K and in the range 0 - 60 GPa [22,23]. The Oganov potential have the form as following

$$V(r_{ij}) = \frac{q_i q_j e^2}{4\pi\varepsilon_0 r_{ij}} + A_{ij}\exp(-B_{ij}r_{ij}) - \frac{C_{ij}}{r_{ij}^6} \qquad (1)$$

where r_{ij} is the distance between i^{th} and j^{th} atoms. The potential parameters A_{ij}, B_{ij}, and C_{ij} are listed in Table 1. We used the Verlet algorithm with a molecular dynamics (MD) time step of 045 femtoseconds (fs). Initially, the model was set up by randomly placing all atoms in a cube and heating it to 6000 Kelvin (K) to remove any potential memory effects. At 6000 K, the model is relaxed for 2×10^5 MD time steps. After that this model is cooled down to 5000, 4000 (at each temperature, the model is also relaxed for 2×10^5 MD time steps) and finally to 3500 K. Next, the model 3500 K is relaxed for a long time (5×10^5 MD time step) in ensemble NPT (constant temperature and pressure) to produce a model at 3500 K and upon ambient pressure, called model M1. Next, different models at temperature of 3500 K and pressures of 5, 10, 15, 20, 25, 30, 40 and 60 GPa are produced by compressing model M1. Each model is relaxed for a long time (6×10^6 MD time step) in ensemble NVE (constant volume and energy). The structural characteristics of each model are determined by averaging over 2000 configurations during the last 2×10^4 MD steps. The cutoff distance used to calculate subnets, bond types, and coordination numbers is determined based on the minimum point after the first peak in the pair radial distribution function (PRDF) $g_{x\text{-}y}(r)$. The cutoff distances chosen are 2.23 Å for SiO bonds and 2.98 Å for MgO bonds.

III. RESULTS AND DISCUSSION

III.1. Structure and structural transition under compression

The PRDFs help us find the average number of atoms at a certain distance, the bond length, the bond angle, and the average number of atoms bonded to a given atom. The six PRDFs that show a disordered structure are in Fig. 1. These functions have a clear first peak and a wider second peak with a lower intensity. The first peak positions for Mg-O, O-O, Si-Si, Mg-Mg, and Si-Mg pairs in $g_{x\text{-}y}(r)$ are located around 160 ± 002, 188 ± 002, 266 ± 002, 308 ± 002, 310 ± 002, and 322 ± 002 Å, respectively, which are in good agreement with experimental measurements reported in ref. [4-6]. To make sure the built models are reliable, their structural properties are checked against experimental data from X-ray diffraction of the molten state. The data show Si-O, Mg-O, and O-O bond length average coordination number, and average bond angles all match the experimental data in refs [5,6] as shown in Table 2.

Fig. 2 displays the distribution of SiO_x and MgO_y (x = 4, 5, 6; y=3, 4,…9) basic units as a function of pressure. As seen, at 0 GPa, about 98% Si atoms have a coordination number of 4. For the distribution of SiO_x, in the range 0-20 GPa, the fraction of SiO_4 decreases, SiO_5 and SiO_6 increases. The fraction of SiO_5 appears the maximum in the range 20-40 GPa, then it decreases with increasing pressure. In contrast, the fraction of SiO_6 continues increasing, and the fraction of SiO_4 continues decreasing with pressure. At 60 GPa, the fractions of SO_4, SiO_5 and SiO_6 are 6, 37 and 55 %, respectively. We conclude that as compressed, the structure of

the SiO network transitions from tetrahedral to octahedral. At low pressure, the SiO network structure consists of SiO_4 clusters. At higher pressure, the Si-O network structure mixes of SiO_4, SiO_5, and SiO_6 clusters. Meanwhile, for the distribution of MgO_y, at ambient pressure, most of the coordination units are MgO_3, MgO_4 and MgO_5. At 60 GPa) comprises MgO_6, MgO_7 and MgO_8. As the pressure increases, the percentage of MgO_3 and MgO_4 units decreases, while the percentage of the other units increases (MgO_5, MgO_6, MgO_7, MgO_8). The fraction of MgO_5 and MgO_6 appears the maximum at about 5 and 15 GPa, respectively and then decreases with pressure. The fraction of MgO_7 and MgO_8 increases as the pressure increases. This means that under compression, there is a low → high Mg-O coordination number transition. As a result, the average Si-O and Mg-O coordination number increases with increasing pressure as seen in Fig. 3. Our analysis shows that the structure of liquid Mg_2SiO_4 changes greatly when it is compressed. Fig. 4 shows the spatial distribution of SiO_x, and MgO_y at 5 GPa and 3500 K. As observed in Fig. 4, SiO_x and MgO_y basic units are linked together into clusters in simulation space.

In order to explain the changes in the Intermediate range order (IRO) and the degree of polymerization in the Mg_2SiO_4 liquid, we consider the characteristics of different types of OT_2 (T is Si or Mg) bonds, triclusters, tetraclusters; Mg-O, Si-O subnets; bridging-, non-bridging-oxygen (BO, NBO) linkages.

Fig. 5 and 6 display the spatial distribution of corner-, edge-, and face-sharing bonds at different pressures. As seen, the distribution of corner-, edge-, and face-sharing bonds is not uniform, instead, they tend to form clusters of corner-, edge- and face-sharing bonds. This again shows the structural heterogeneity of Mg_2SiO_4 liquid. It can be also shown that edge- and face-sharing bonds are mainly between TO_5 and TO_6 units. It means that the clusters of edge- and face-sharing bonds will form high-density regions. This also demonstrates that there exists structural heterogeneity in Mg_2SiO_4 liquid. Both figures show the presence of structures that are either Si-rich or Mg-rich. Moreover, the increase in corner-, edge-, and face-sharing can also be observed as pressure increases.

The number distributions of corner-, edge- and face -sharing bonds are listed in Table 3. As seen, all corner-, edge-, and face -sharing bonds increase with increasing pressure. For SiO_x–SiO_y links, corner-sharing bonds account for dominant bonds, meanwhile, edge-sharing bonds account for small bonds and face-sharing bonds. In which SiO_4–SiO_4 links only contain corner-sharing bonds while both corner- and edge-sharing bonds comprise SiO_4–SiO_5, SiO_4–SiO_6, and SiO_5–SiO_5 links. For MgO_x–MgO_y and SiO_x–MgO_y links, corner-sharing bonds also account for dominant but edge-sharing bonds are significant. Also, a few ten face-sharing bonds appear in these links. We also found that face-sharing bonds comprise in MgO_5–MgO_5, MgO_5–MgO_6, SiO_5–MgO_5, and SiO_5–MgO_6 links and edge-sharing bonds comprise in all links except ones connected with MgO_3 unit. There are some significant differences in the links among SiO_x and links among MgO_y units.

III.2. Degree of polymerization under compression

To further clarify the degree of polymerization under compression, we examined the number of OT_2, triclusters, tetraclusters bonds, the distribution of BO and NBO in SiO_x units, and the number of Si-O and Mg-O subnets. The BO is the one that bonds to at least two Si atoms, other bonds are NBO.

As seen in Fig. 7, the number of OT_2 bonds decreases, in contrast, triclusters and tetraclusters increase with pressure. The number of triclusters also appears the maximum in the range 28-30 GPa as seen in the distribution of SiO_5 units, then it decreases with the pressure increasing (see Fig. 7a). Fig. 7b shows that pressure increases from 0 to 60 GPa, the number of BO and MgO_y-SiO_x linkages increases continuously, and in contrast, NBO linkages decrease. It also means that under compression, SiO_x units tend to form clusters in space. Also, this result demonstrates that the degree of polymerization increases with pressure.
On the other hand, Fig. 8 shows that the number of Mg-O, and Si-O subnets significantly decreases under compression. The number of Si-O subnets is three times smaller than Mg-O. Unlike the SiO_x units, MgO_y does not lend to form clusters. It again confirms that SiO_x units form a network structure in Mg_2SiO_4 liquid. This result means that the degree of polymerization increases with pressure. Most of all Si atoms are the main network-former in Mg_2SiO_4 liquid.

III.3. Dynamics characteristics in Mg_2SiO_4 liquid

Dynamics properties as self-diffusions in the Mg_2SiO_4 liquid were analyzed through the mean square displacement (MSD) of atoms. Fig. 9 shows the time dependence of MSD of Si, O, and Mg atoms at some different pressures. The plots of MSD show a diffusive regime as a first-order function of time. The mean square displacement (MSD) of all atom types is calculated through analysis of each atom's trajectory from the simulation time step. MSD_X of X-atom as a function of time steps is presented by the following equation

$$MSD_X = \frac{\sum [r_{Xi}(t) - r_{Xi}(0)]^2}{N_{Xi}} \qquad (2)$$

Where $r_{Xi}(0)$ and $r_{Xi}(t)$ is the position of atoms at time $t = 0$ and t, respectively, N_{Xi} the number of atoms of type X. The self-diffusion coefficients D_X of X-atom were calculated from the slope of MSD_X and follow equation Einstein below

$$D_X = \lim_{t \to \infty} \frac{MSD_X}{6t} \qquad (3)$$

Using eq. (3), the self-diffusion coefficients of Si, O, and Mg atoms are calculated as seen in Table 4. We find that the diffusivity of O, Si, and Mg atoms decreases with increased pressure. This happens because the polymerization of Mg_2SiO_4 liquid increases under pressure. In considered pressure, we show that $D_{Si} < D_O < D_{Mg}$. Table 4 shows that the results of the coefficients are similar to data from previous experiments and simulations as seen in refs. [7,24,25]. In addition, it can be seen that in the low-pressure range, the diffusion coefficient of Mg atoms equals two times one of Si or O atoms. Fig.10 displays the distribution of 5% of sets of slowest atoms (SSA) and fastest atoms (SFA) in the Mg_2SiO_4 liquid at 3500 K and 0 GPa. As seen, both the fastest and slowest atoms tend to form clusters, and the distributions are not uniform. The SFA are distributed by mainly Mg atoms, meanwhile, the SSA are distributed by mainly O and Si atoms. This demonstrates that the

dynamics of atoms is heterogeneous, and Mg atoms diffuse the fastest in liquid. The fast diffusion of Mg atoms in a low-pressure range can be explained through the diffusion channels created by the boundary of the Mg- and Si-rich regions. As shown Fig. 11, the Mg atoms are mainly localized beyond the cluster of SiO_x-SiO_y. It means that Mg atoms are more mobile than Si and O atoms. It can be shown in Fig. 11, several channels (cross-sections) where all atoms are shown, and the Mg atoms near each other are highlighted in blue. It is noted that the size and location of these channels insignificantly change over time.

4. CONCLUSION

We carry out the MD simulations for models of Mg_2SiO_4 liquid at 3500 K, in a wide pressure range of 0-60 GPa. Several conclusions can be drawn as follows

- The structure of Mg_2SiO_4 liquid comprises MgO_y basic units distributed in Si-O network structure. Mg-O, Si-O subnets lend to form a structural heterogeneity. The structure of Mg_2SiO_4 liquid significantly changes under compression. Namely, there is a tetrahedral → octahedral structure transition in Si-O network structure, and a low → high Mg-O coordination number transition with increased pressure.

- Under compression, the structural transitions of Mg_2SiO_4 liquid mainly relate the change of IRO, meanwhile, SRO is not sensitive to compression. We find that under compression, the degree of polymerisation significantly increases.

- In considered pressure, we find that $D_{Si} < D_O < D_{Mg}$. We conclude that the dynamics of atoms is heterogeneous. In the low-pressure range, Mg atoms diffuse the fastest in liquid. The fast diffusion of Mg atoms in a low-pressure range can be explained through the diffusion channels created by the boundary of the Mg- and Si-rich regions.

REFERENCES

[1] O.O. Taspinar, S. Ozgul-Yucel, Lipid adsorption capacities of magnesium silicate and activated carbon prepared from the same rice hull, Eur. J. Lipid Sci. Technol. 110 (2008) 742–746.

[2] I. Rashid, N.H. Daraghmeh, M.M. Al Omari, B.Z. Chowdhry, S.A. Leharne, H. A. Hodali, A.A. Badwan, Profiles of Drug Substances, Excipients and Related Methodology, vol. 36, Academic Press, 2011.

[3] K. Yanagisawa, K. Masaki, K. Someno, Method for Producing Rubber-Filler Master Batch, US20090018238A1, 2009.

[4] A. Takashi, A. Ryuichi, S. Mamoru, M. Naoya, M. Megumi, S. Masako, Recording Paper and Ink Jet Recording Method by Use Thereof, US4758461, 1988.

[5] Kohara S., Suzuya K., Takeuchi K., Loong C. K., Grimsditch M., Weber J. K. R., Tangeman J. A. and Key T. S. (2004) Glass formation at the limit of insufficient network formers. Science 303, 1649–1652.

[6] de Koker, N. P., Stixrude, L., & Karki, B. B. (2008). Thermodynamics, structure, dynamics, and freezing of Mg_2SiO_4 liquid at high pressure. Geochimica et Cosmochimica Acta, 72(5), 1427-1441.

[7] Adjaoud, O., Steinle-Neumann, G., & Jahn, S. (2008). Mg_2SiO_4 liquid under high pressure from molecular dynamics. Chemical Geology, 256(3-4), 185-192.
[8] Cochain, B., Sanloup, C., Leroy, C., & Kono, Y. (2017). Viscosity of mafic magmas at high pressures. Geophysical Research Letters, 44(2), 818-826.
[9] Taniguchi, T., Okuno, M., & Matsumoto, T. (1997). X-ray diffraction and EXAFS studies of silicate glasses containing Mg, Ca and Ba atoms. Journal of non-crystalline solids, 211(1-2), 56-63.
[10] Wilding, M. C., Benmore, C. J., Tangeman, J. A., & Sampath, S. (2004). Coordination changes in magnesium silicate glasses. Europhysics Letters, 67(2), 212-218.
[11] Wilding, M. C., Benmore, C. J., Tangeman, J. A., & Sampath, S. (2004). Evidence of different structures in magnesium silicate liquids: coordination changes in forsterite-to enstatite-composition glasses. Chemical Geology, 213(1-3), 281-291.
[12] Fiske, P.S., Nellis, W.J., Xu, Z., Stebbins, J.F., 1998. Shocked quartz; a 29Si magic-angle spinning nuclear magnetic resonance study. Am. Mineral. 83, 1285–1292
[13] Allwardt, J.R., Stebbins, J.F., Terasaki, H., Du, L.-S., Frost, D.J., Withers, A.C., Hirschmann, M.M., Suzuki, A., Ohtani, E., 2007. Effect of structural transitions on properties of high-pressure silicate melts: ^{27}Al NMR, glass densities, and melt viscosities. Am. Mineral. 92, 1093–1104
[14] Kelsey, K.E., Stebbins, J.F., Du, L.-S., Hankins, B., 2007. Constraining ^{17}O and ^{27}Al NMR spectra of high-pressure crystals and glasses: new data for jadeite, pyrope, grossular, and mullite. Am. Mineral. 92, 210–216
[15] Dobson, D. P., Dohmen, R., & Wiedenbeck, M. (2008). Self-diffusion of oxygen and silicon in $MgSiO_3$ perovskite. Earth and Planetary Science Letters, 270(1-2), 125-129.
[16] Zhang, B., Wu, X., & Zhou, R. (2011). Calculation of oxygen self-diffusion coefficients in Mg_2SiO_4 polymorphs and $MgSiO_3$ perovskite based on the compensation law. Solid State Ionics, 186(1), 20-28.
[17] Reid, J.E., Suzuki, A., Funakoshi, K., Terasaki, H., Poe, B.T., Rubie, D.C., Ohtani, E., 2003. The viscosity of $CaMgSi_2O_6$ liquid at pressures up to 13 GPa. Phys. Earth Planet. Inter. 139, 45–54
[18] Liebske, C., Schmickler, B., Terasaki, H., Poe, B.T., Suzuki, A., Funakoshi, K., Ando, R., Rubie, D.C., 2005. Viscosity of peridotite liquid up to 13 GPa: Implications for magma ocean viscosities. Earth Planet. Sci. Lett. 240, 589–604.
[19] Stixrude, L., Karki, B., 2005. Structure and freezing of $MgSiO_3$ liquid in Earth's lower mantle. Science 310, 297–299
[20] Karki, B.B., Bhattarai, D., Stixrude, L., 2006. First-principles calculations of the structural, dynamical, and electronic properties of liquid MgO. Phys. Rev. B 73,174208 (7 pages).
[21] Karki, B.B., Bhattarai, D., Stixrude, L., 2007. First-principles simulations of liquid silica: Structural and dynamical behavior at high pressure. Phys. Rev. B 76,104205 (12 pages).
[22] Nevins, D., Spera, F. J., & Ghiorso, M. S. (2009). Shear viscosity and diffusion in liquid $MgSiO_3$: Transport properties and implications for terrestrial planet magma oceans. *American Mineralogist*, *94*(7), 975-980.
[23] Oganov, A. R., Brodholt, J. P., & Price, G. D. (2000). Comparative study of quasiharmonic lattice dynamics, molecular dynamics and Debye model applied to $MgSiO_3$ perovskite. *Physics of the Earth and Planetary Interiors*, *122*(3-4), 277-288.

[24] Lacks, D. J., Rear, D. B., & Van Orman, J. A. (2007). Molecular dynamics investigation of viscosity, chemical diffusivities and partial molar volumes of liquids along the $MgO–SiO_2$ join as functions of pressure. *Geochimica et Cosmochimica Acta*, *71*(5), 1312-1323.
[25] Spera, F. J., Ghiorso, M. S., & Nevins, D. (2011). Structure, thermodynamic and transport properties of liquid $MgSiO_3$: Comparison of molecular models and laboratory results. *Geochimica et Cosmochimica Acta*, *75*(5), 1272-1296.
26. Zhou, L., Xue, W., & Zeng, Z. (2016). Isothermal Crystallizaiton Kinetic and Melting Behaviors of Nylon 6/66/510. Chemical Science International Journal, 14(1), 1–10. https://doi.org/10.9734/ACSJ/2016/25442
27. Ahmad Mir, M., Ahmad Naikoo, R., Bhat, S., Tomar, R., Ahmad Bhat, M., Ahmad Bhat, R., Dipak, P., & C. Tiwari, D. (2016). Effect of Different Variables on the Electrical Conductivity Sensitivity of Synthesized Zeolite/Polymer Composites for Various Gases: A Review. Chemical Science International Journal, 13(2), 1–18. https://doi.org/10.9734/ACSJ/2016/23558

THE TABLES

Table 1. The parameters of Oganov potential [22,23]

i	j	A_{ij} (eV)	B_{ij} (Å)	V_{ij} (Å^6)	q (eC)
Mg	Mg	0	0	0	q_{Si} = 2.9043
Mg	Si	0	0	0	q_{Mg} = 1.9104
Mg	O	1041.43266	3.48918	0	q_O = -1.6049
Si	Si	0	0	0	–
Si	O	1137.02499	3.53732	0	–
O	O	2023.79522	3.73972	3.30544	–

Table 2. Inter-atomic distance (Å)

P (GPa)	r_{SiSi}	r_{SiO}	r_{OO}	r_{SiMg}	r_{OMg}	r_{MgMg}
0	3.10	1.56	2.66	3.16	1.88	3.22
5	3.04	1.56	2.62	3.22	1.90	3.00
10	3.08	1.56	2.56	3.06	1.94	3.00
15	3.04	1.56	2.56	3.08	1.92	2.86
20	3.04	1.56	2.56	3.02	1.90	2.86
25	3.02	1.58	2.58	2.96	1.90	2.82
30	3.06	1.58	2.50	2.92	1.88	2.82
40	2.98	1.58	2.44	2.88	1.90	2.80
60	3.00	1.60	2.46	2.78	1.90	2.72
Exp. [5]	–	1.63	–	–	2.00	–
Simu. [6]	–	1.64-1.62	–	–	1.97-1.83	–

Table 3. The distributions of connectivities in the models; Nc, Ne, and Nf are the number of corner-, edge-, and face-sharing bonds

P (GPa)	MgO_x-MgO_y			MgO_x-SiO_y			SiO_x-SiO_y		
	Nc	Ne	Nf	Nc	Ne	Nf	Nc	Ne	Nf
0	2639	504	29	2504	576	96	504	25	0
5	3246	871	63	3124	749	157	565	41	3
10	3562	1116	133	4031	966	239	658	87	4
15	3810	1306	205	4403	1203	330	661	124	16
20	3915	1561	302	5384	1316	485	751	165	14
25	4054	1690	390	6027	1493	571	804	172	21
30	4207	1883	502	6870	1793	702	857	231	26
40	4278	2043	640	7737	2038	945	894	272	46
60	4281	2385	829	9351	2551	1167	942	316	46

Table 4. The self-diffusion constant for Si, O, and Mg atoms

P (GPa)	0	5	10	15	20	25	30	40	60	References
D_{Si} ×10^{-6} (cm^2/s)	4.01	3.54	2.89	2.74	2.31	2.19	1.72	1.24	0.62	3.35[a]; 2.50[b]
D_O ×10^{-6} (cm^2/s)	5.28	4.78	4.20	3.78	3.37	3.08	2.39	1.73	0.86	5.48[a]; 5.30[b]
D_{Mg} ×10^{-6} (cm^2/s)	11.39	8.24	6.11	5.28	4.61	4.06	3.07	2.31	1.21	10.5[a]

[a, b] Simulation data is given in refs. [7], [24], respectively.

THE FIGURES

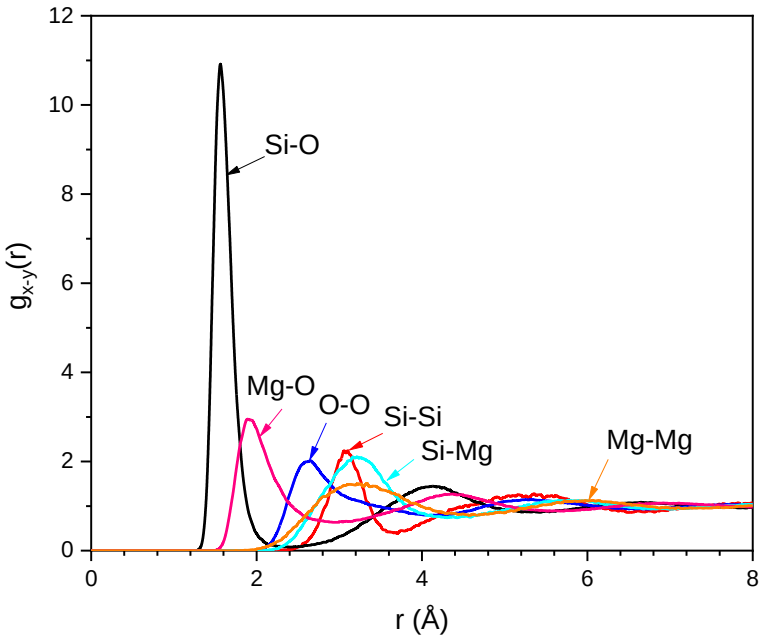

Fig. 1. The PRDFs of Si-O, Mg-O, O-O, Si-Si, Si-Mg, and Mg-Mg pairs in the Mg_2SiO_2 model at 3500 K and 0 GPa.

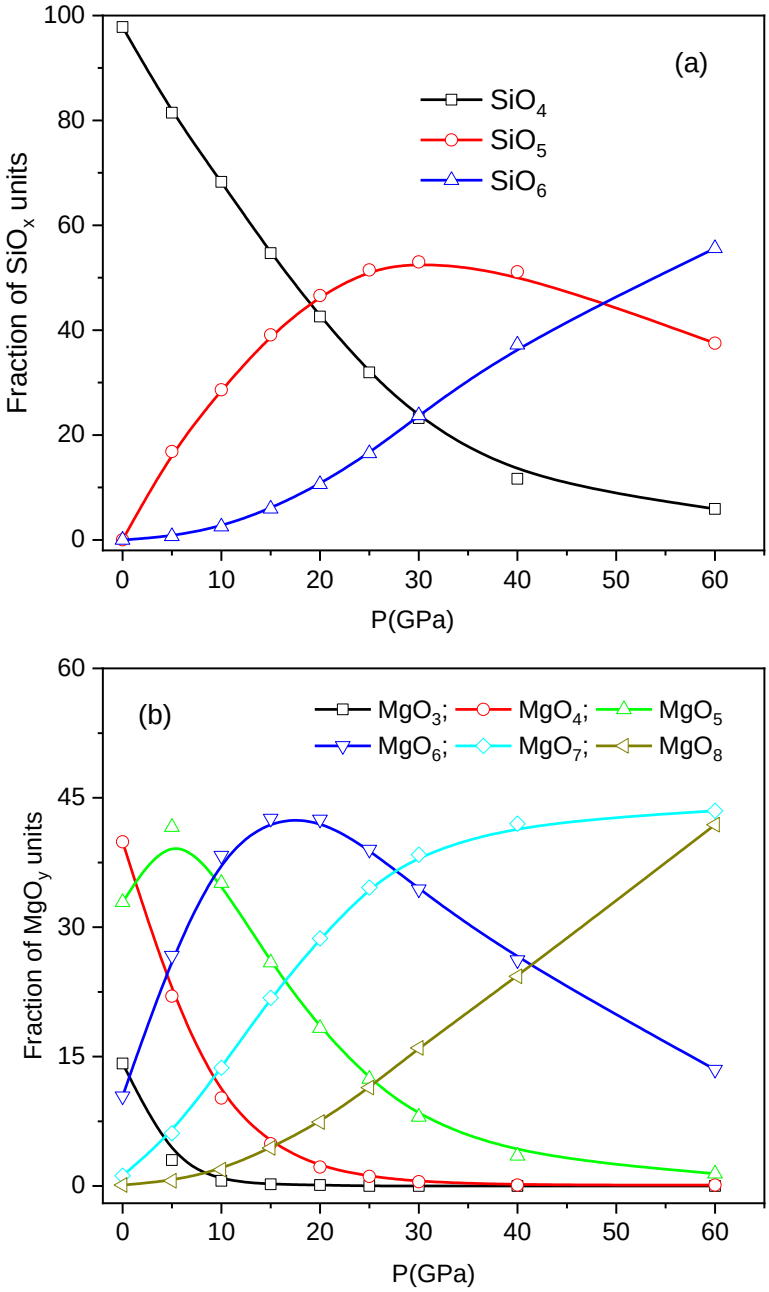

Fig. 2. The dependence of the fraction of basic units as a function of pressure: (a) displays the fraction of SiO_4, SiO_5, and SiO_6 units, (b) displays the fraction of MgO_3, MgO_4,… MgO_8 units.

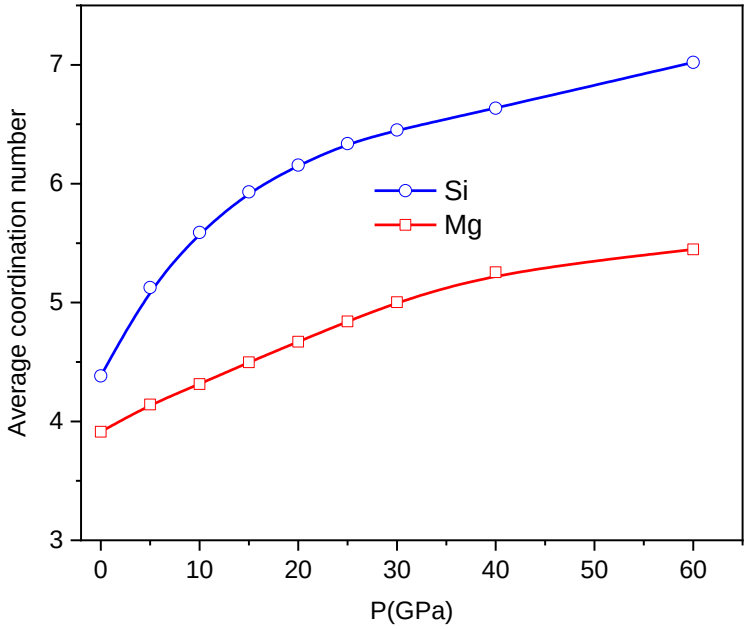

Fig. 3. The Si-O and Mg-O atoms average coordination number distribution as a function of pressure.

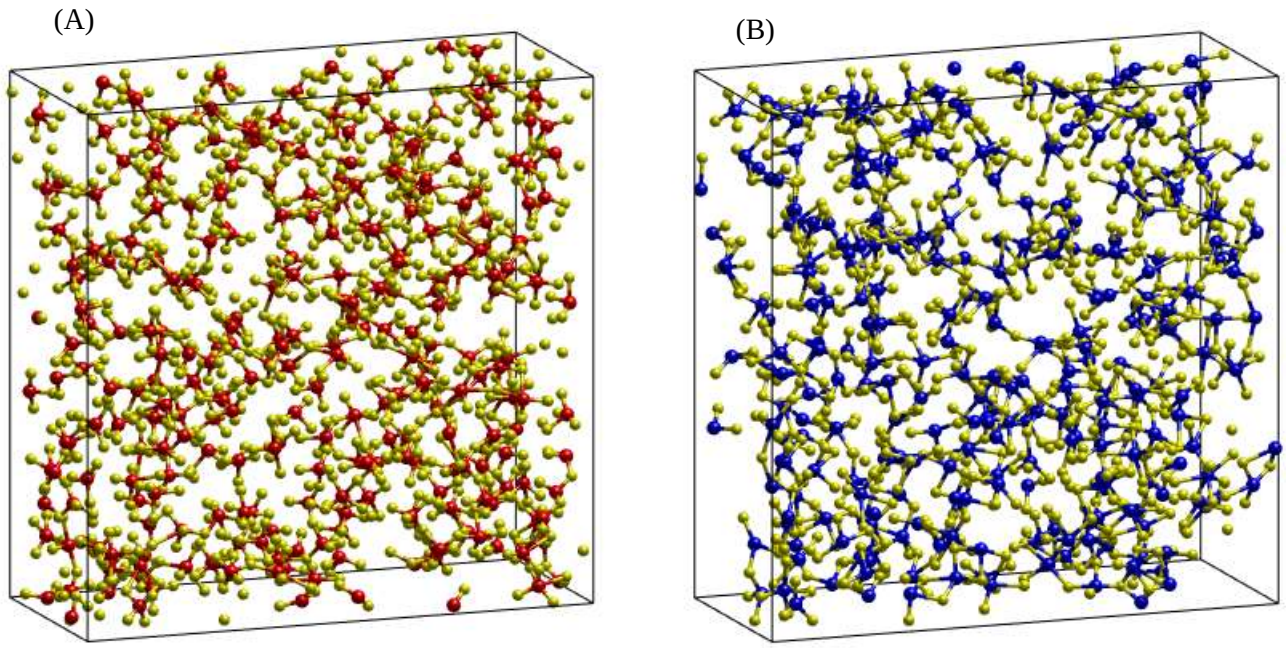

Fig. 4. Spatial distribution of SiO_4, SiO_5, and SiO_6 (A); MgO_3, MgO_4, MgO_5, MgO_6, MgO_7 and MgO_8 (B) at 5 GPa, 3500 K. Here Si, Mg, and O atom are red, blue, yellow balls, respectively.

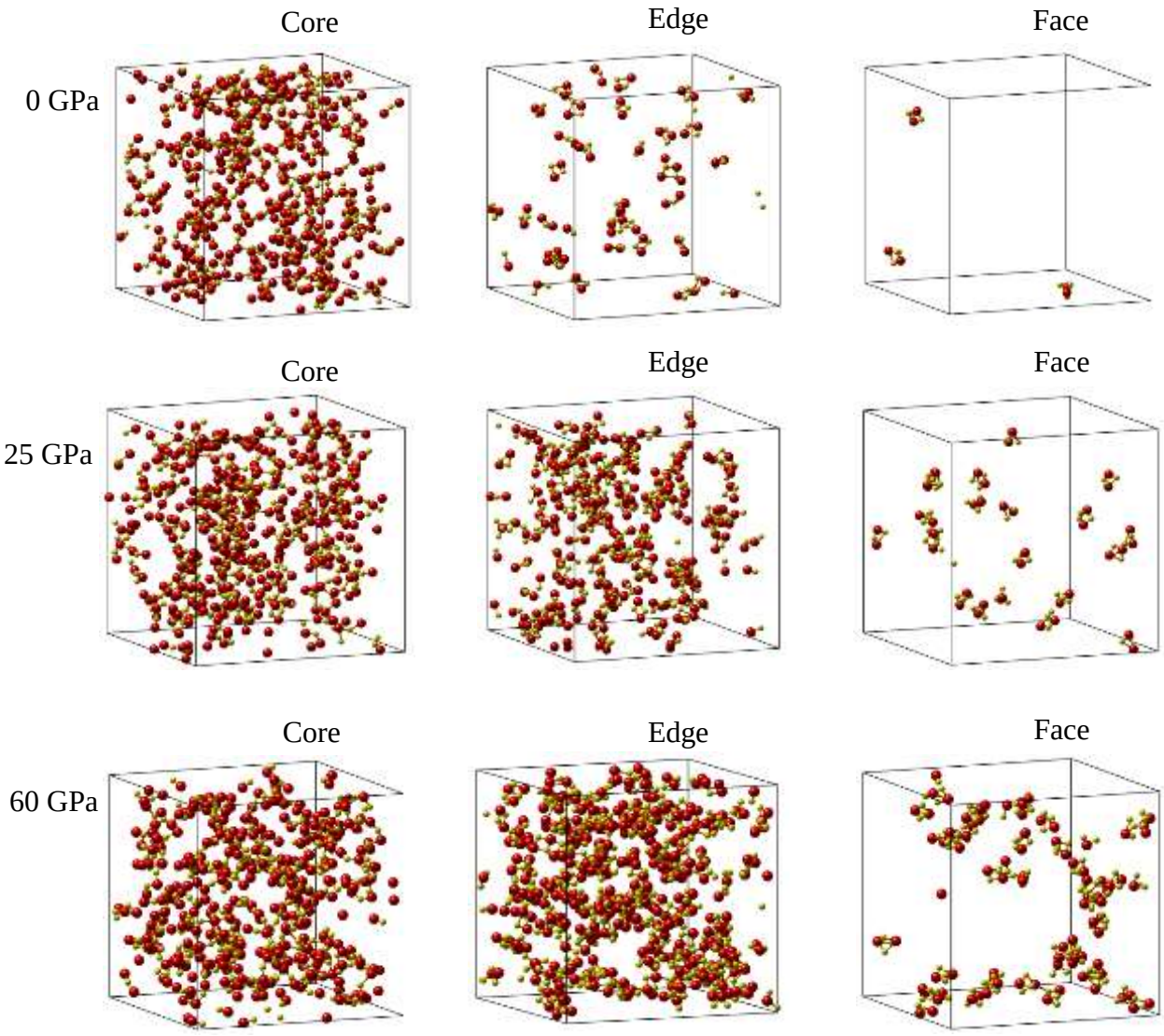

Fig. 5. Spatial distribution of SiO_x-SiO_y pairs connected through one, two, and three common oxygen atoms (core-, edge-, face -sharing) at pressures 0, 25, and 60 GPa. Here Si and O atoms are red, and yellow balls, respectively.

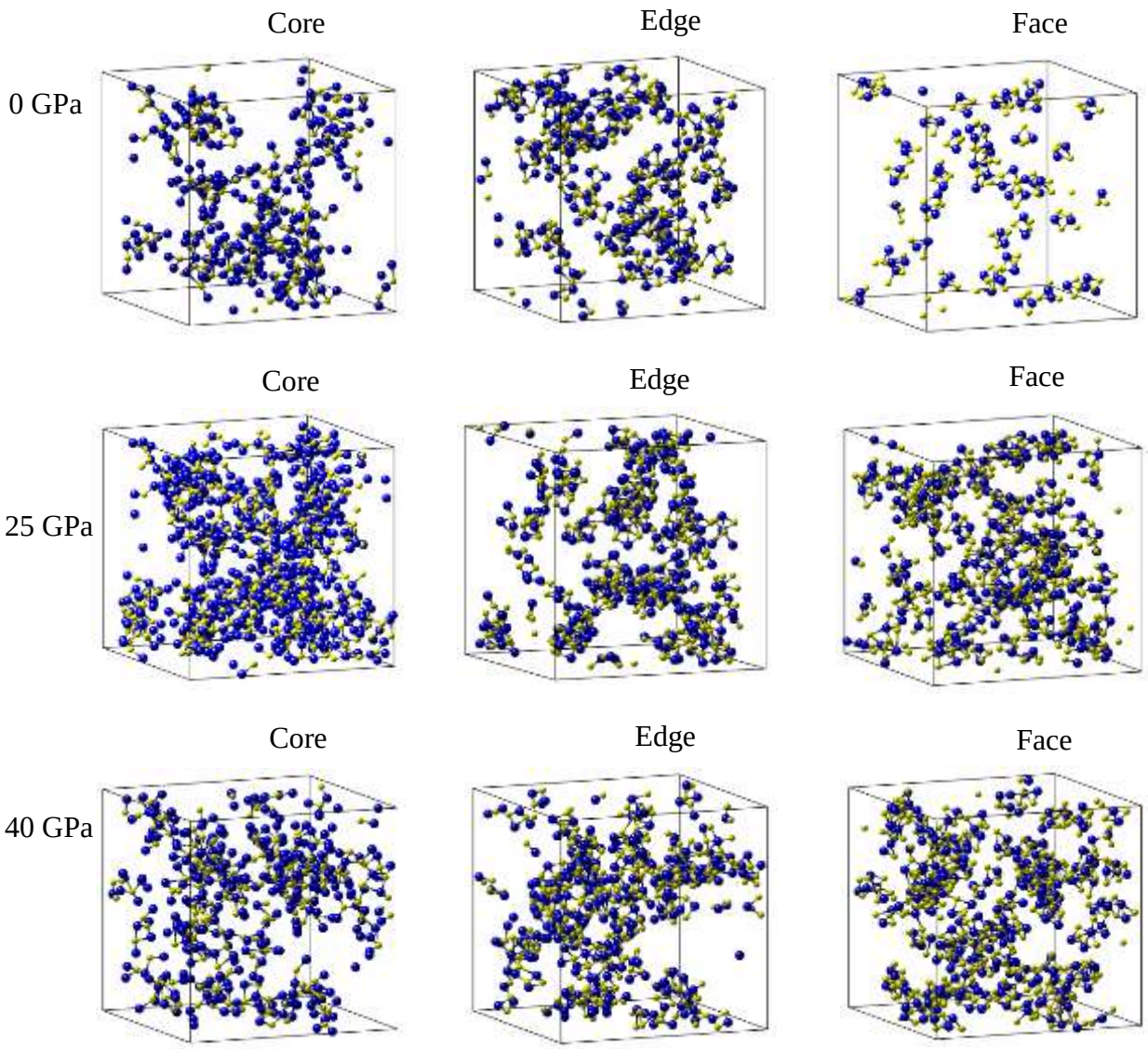

Fig. 6. Spatial distribution of MgO_x-MgO_y pairs connected through one, two, and three common oxygen atoms (core-, edge-, face- sharing) at pressures 0, 25, and 40 GPa. Here Mg and O atoms are blue, and yellow balls, respectively.

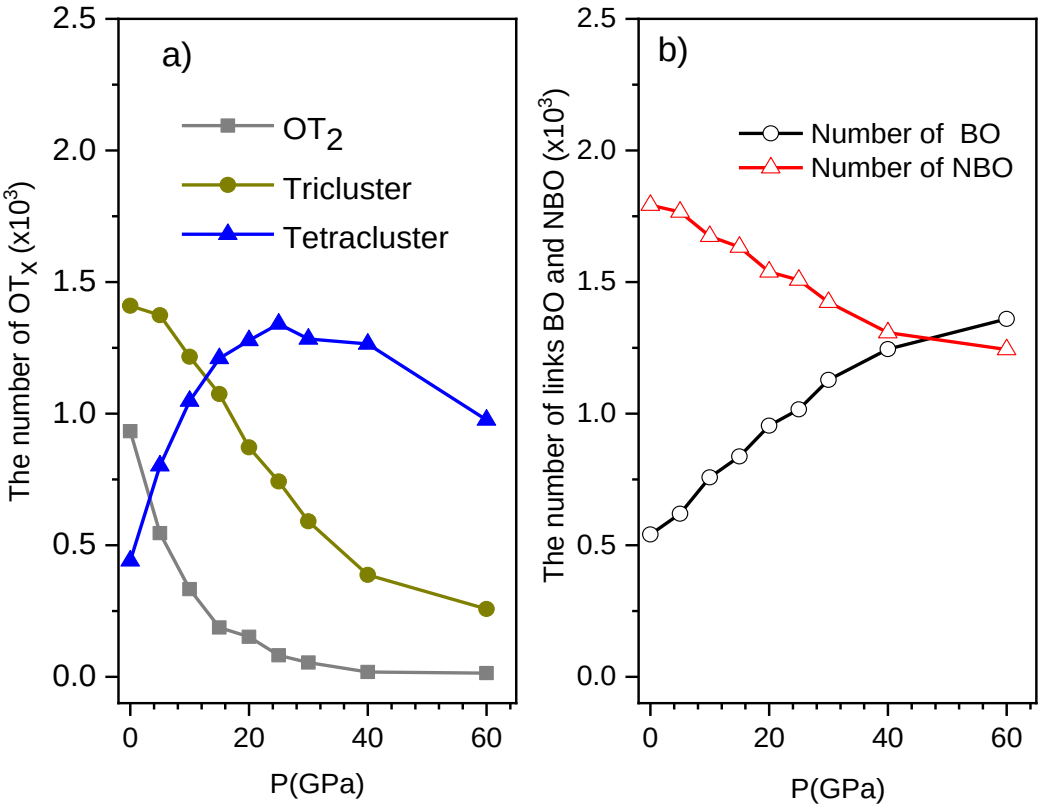

Fig. 7. The number of OT_2 (T is Si or Mg), triclusters, and tetraclusters (a), links of BO and NBO (b) such as a function of pressure.

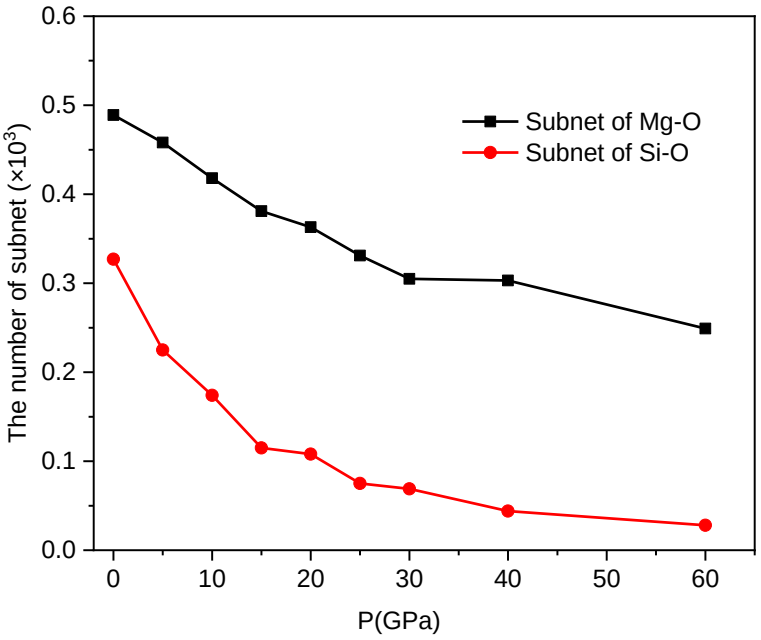

Fig. 8. The number of Si-O and Mg-O subnets such as a function of pressure

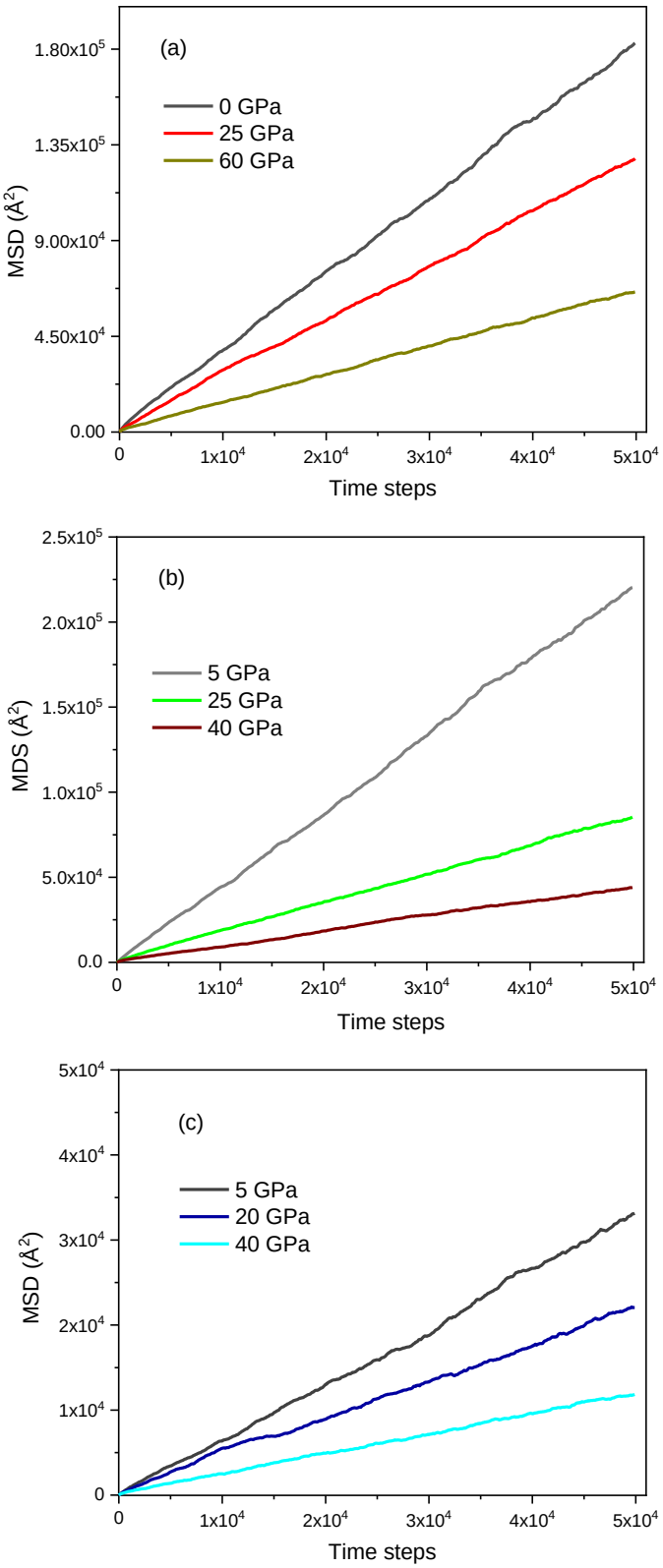

Fig. 9. MSD of O (a), Mg (b), and Si (c) atoms as a function of simulation time steps at some different pressures.

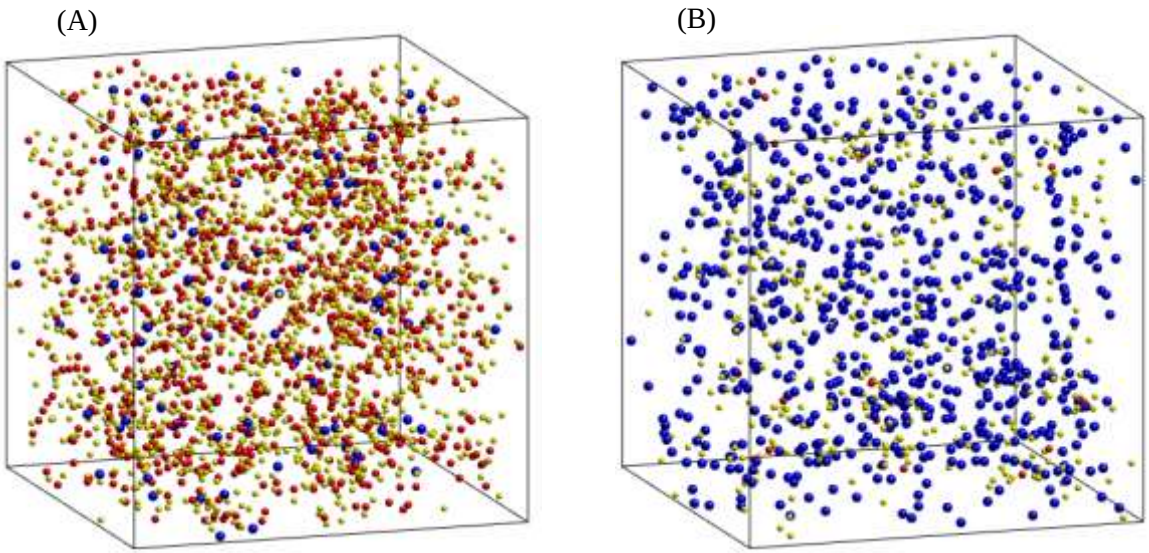

Fig. 10. (A) The distribution of 5 % of sets of slowest atoms (SSA) and (B) fastest atoms (SFA) at 3500 K and 0 GPa. The red ball is Si, the blue ball is Mg, and the yellow ball is O.

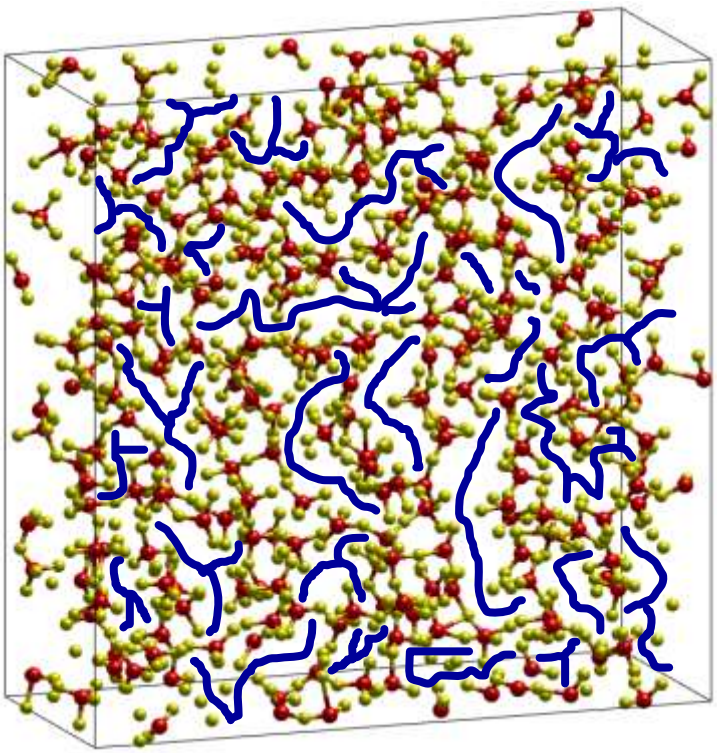

Fig. 11. Schematic illustration of some channel for a typical spatial distribution of the atoms at 0 GPa and 3500 K. Here, in blue highlight are the Mg - diffusion pathways; Si, and O are red and yellow balls, respectively.